Fusion Induced By Medium-Mass Radioactive Ion Beams

J. F. Liang

Physics Division, Oak Ridge National Laboratory, Oak Ridge, TN 37831, U.S.A.

Abstract. The use of radioactive ion beams in nuclear physics experiments has increased rapidly in recent years. A variety of short-lived nuclei and beam energies are available. With medium-mass, neutron-rich radioactive nuclei, the influence of neutron excess on fusion and compound nucleus survival can be explored. This can improve our understanding on how to synthesize new neutron-rich heavy nuclei. Fusion induced by medium-mass, neutron-rich radioactive nuclei, ^{38}S, ^{132,134}Sn, and ^{134}Te has been measured. Enhanced fusion cross sections were observed in these measurements. However, in most of the cases the enhancement is due to the lowering of the barrier by the larger nuclear sizes except for ^{134}Sn induced fusion. Results from these experiments and future plans are discussed.

Keywords: radioactive ion beam, fusion, fission, evaporation residue
PACS: 25.70.-z, 25.70.Jj

INTRODUCTION

It is predicted that sub-barrier fusion would be enhanced in reactions involving neutron-rich radioactive nuclei. The enhancement is in part because of the larger radius of the radioactive nuclei which lowers the barrier. Neutron-rich RIBs provides opportunities to study the influence of neutron transfer on fusion[1, 2]. The number of neutron transfer channels with positive Q-values can be very large for certain radioactive beam and stable target combinations. The transfer of neutrons as a flow of neutrons may occur in such reactions and subsequently result in fusion enhancement. Furthermore, the compound nucleus formed in such reactions is expected to have a higher survival probability because of the decreased fissility and longer lifetimes.

Measurements of fusion using neutron-rich radioactive beams have been pursued in laboratories worldwide. The goal is to study the reaction mechanisms that contribute to the fusion enhancement and be able to reliably predict cross sections of fusion induced by neutron-rich radioactive beams. It is anticipated that new, neutron-rich isotopes of the heaviest elements can be produced with such beams at next generation radioactive beam facilities. With the increased lifetimes of these isotopes, the chemical properties of heavy elements can be studied.

This report discusses recent experiments (2004 to present) carried out with medium-mass neutron-rich radioactive beams. A review of earlier measurements can be found in Ref. [3].

EXPERIMENTAL METHODS

At present, the intensity of RIBs is at most 10^8 particles per second (pps). Typically it is between 10^3 and 10^6 pps. In contrast, the intensity of stable beams is measured in terms of beam current where one particle nanoAmpere is 6.25×10^9 pps. It is obvious that high efficiency detectors are required to optimize the counting rate. Figure 1 shows two examples of detectors for measuring fusion reactions induced by RIBs. The compound nucleus can decay by particle evaporation and fission. An ionization chamber located at zero degrees for identifying evaporation residues (ER) by the energy loss of particles is shown in Fig. 1(a). The timing channel plate detectors are used for time-of-flight measurements and counting the beam particles for normalization. Fission fragments can be detected by an annular silicon strip detector or an array of large area silicon strip detectors as shown in Fig 1(a) and 1(b), respectively. Sometimes a thick target[4] or a stack of targets[5] are used to compensate for the low beam intensity.

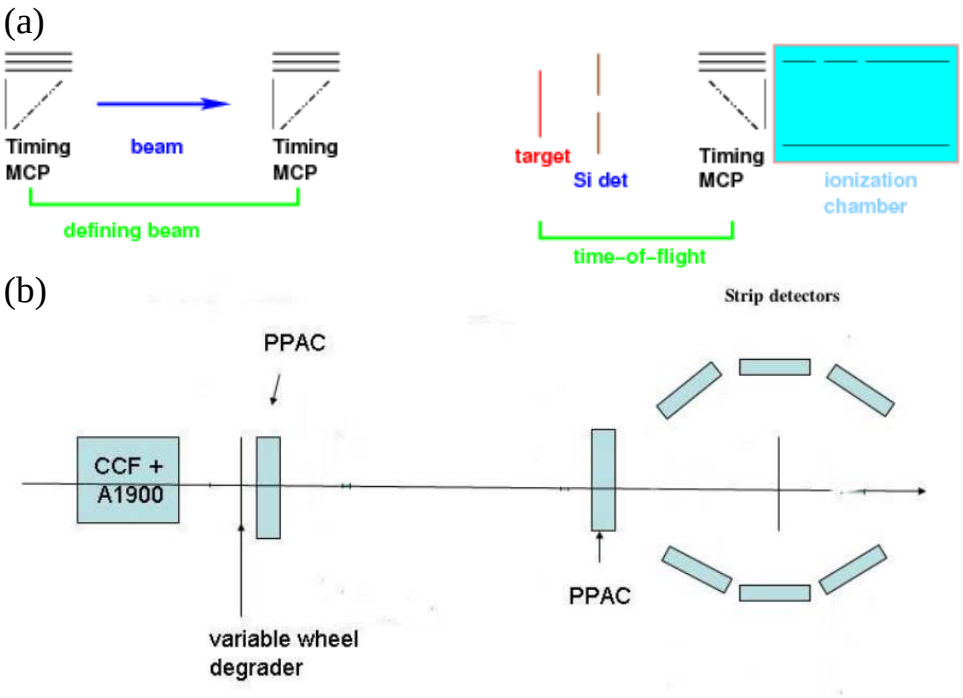

FIGURE 1. Examples of apparatus for measuring (a)ERs and fission, and (b)fission.

FUSION INDUCED BY ^{38}S

The fission excitation function was measured for ^{38}S+^{208}Pb and compared to that for ^{32}S on the same target by an Oregon State University group[6]. This is an extension of their study of the ^{38}S+^{181}Ta fusion-fission reaction[7, 8]. The main conclusion from both experiments is that the fusion induced by ^{38}S is enhanced with respect to that induced by ^{32}S. However, the fusion enhancement can be accounted for by the larger radius of ^{38}S lowering the barrier. Shown in Fig. 2(a) is a comparison of the fission excitation

function of ^{38}S and ^{32}S on ^{208}Pb. The fission cross sections for ^{38}+^{208}Pb are apparently larger than those for ^{32}S+^{208}Pb[9, 10]. If the nuclear sizes and the shift of barriers due to the change in nuclear sizes are considered, the enhancement observed in ^{38}S induced fusion with respect to ^{32}S induced fusion is absent. This is shown in Fig. 2(b) where the nuclear size (radius squared) and the barrier shift of the reacting nuclei are factored out in the reduced cross section and reduced energy, respectively.

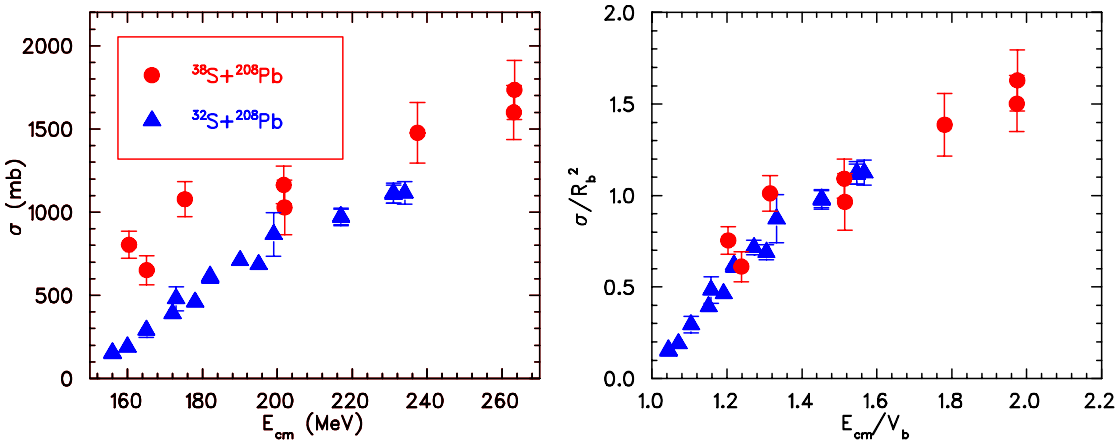

FIGURE 2. (a)Fission excitation functions for ^{32}S+^{208}Pb (triangles) and ^{38}S+^{208}Pb (circles). (b)Reduced fission excitation functions for ^{32,38}S+^{208}Pb where the nuclear size and barrier are factored out for cross section and energy axes, respectively.

It can be seen in Fig. 2(b) that the measurement of ^{38}S+^{208}Pb was performed at energies above the barrier. It would be interesting to extend the measurement to energies below the barrier because fusion enhancement because of channel-couplings often occurs at sub-barrier energies.

The uncertainty of the data is fairly large. The is in part because of the quality of the beam. The ^{38}S beam was produced by the fragmentation of a 140 MeV/A ^{40}Ar beam at Michigan State University. The ^{38}S was tuned through a sophisticated fragment separator (A1900) and degraded to 8 MeV/A. The energy of the beam was subsequently reduced to the desired energies by some variable degrader foils mounted at the entrance of the scattering chamber. As a result, the emittance of the beam was very poor and a collimator was installed in front of the target to reduce the beam spot size. Moreover, the width of the beam energy was 20 MeV (FWHM). Even with the utilization of beam tagging, the impact of beam degradation on the data quality is severe. This makes measurement at energies below the barrier more difficult.

^{132,134}SN AND ^{134}TE INDUCED FUSION

I. ^{64}Ni target

Accelerated neutron-rich radioactive beams from proton-induced uranium fission are available at the Holifield Radioactive Ion Beam Facility. The doubly magic ^{132}Sn has been used for nuclear structure and nuclear reaction studies. The fusion excitation function of ^{132}Sn+^{64}Ni has been measured. The ER and fission cross sections as a function of

energy are shown by the open and filled circles, respectively, in Fig. 3. Statistical model calculations, using the code PACE2[11] with parameters simultaneously fitting ER and fission cross sections for ^{64}Ni on all even stable Sn isotopes, are in good agreement with the data.

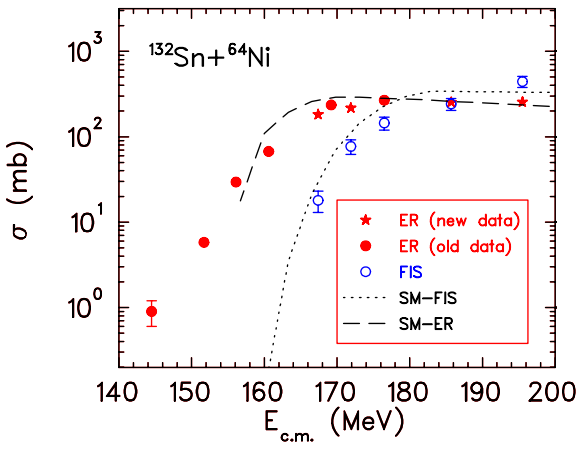

FIGURE 3. Excitation functions of ER (filled circles and stars) and fission (open circles) for ^{132}Sn+^{64}Ni. The dashed and dotted curves are statistical model predictions of ER and fission cross sections, respectively. .

Figure 4 presents a comparison of the measured fusion, the sum of ER and fission, excitation function to a one-dimensional barrier penetration model prediction (dotted curve). A larger sub-barrier fusion enhancement is observed. The coupled-channel calculations are performed using the code CCFULL[12] with potential parameters from Broglia-Winther systematics[13]. The dashed curve is the result of calculations including the excitation to the lowest 2^+ state in ^{132}Sn, and 2^+ and 3^- states in ^{64}Ni. The calculations overpredict the measured cross sections near the barrier but underpredict the data below the barrier. It is noted that the Q-value is positive for transferring two to six neutrons from Sn to Ni. The result of calculations considering the coupling of inelastic excitation and transfer reproduces the data very well. The transfer coupling constant is arbitrarily set to equal 0.35 to reproduce the data. Also shown in the figure is a microscopic model, Skyrme Energy Density Functional, prediction (solid curve)[14] which over estimates the data at all energies.

The ER excitation function of ^{132}Sn+^{64}Ni is compared to that of ^{124}Sn+^{64}Ni[15] as shown in Fig. 5. The barrier height for the two systems predicted by the Bass model[16] is also shown in the figure. At energies less than 160 MeV, fission is predicted to be negligible by PACE2. Therefore, the ER cross sections are taken as fusion cross sections for $E_{cm} < 160$ MeV. It can be seen that fusion induced by ^{132}Sn is enhanced at sub-barrier energies as compared to that induced by ^{124}Sn. However, the enhancement can be accounted for by the barrier shift due to the larger radius of ^{132}Sn.

To compare the ER formed in the reactions of ^{64}Ni on Sn isotopes[17], the dimensionless reduced ER cross section, $\bar{\sigma}_{ER}$, is used. The reduced ER cross section is defined as the ER cross section divided by the kinematic factor, $\pi\lambda\!\!\!^{-2}$. Figure 6(a) displays the reduced ER cross section as a function of the center of mass energy. It can be seen that the reduced ER cross section increases as the center of mass energy increases and saturates as fission becomes a significant fraction of the fusion cross section. The saturation

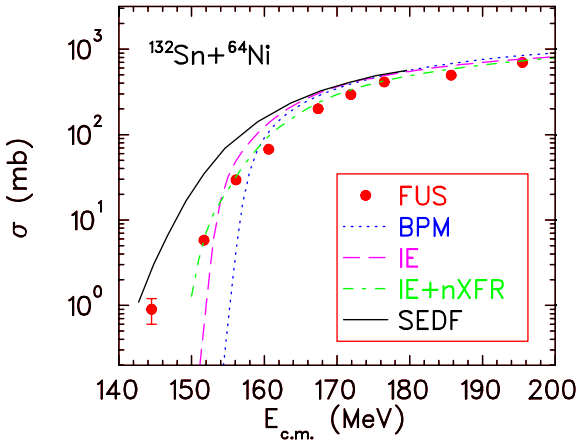

FIGURE 4. Comparison of measured ^{132}Sn+^{64}Ni fusion cross sections (filled circles) with coupled-channel calculations. The result of one dimensional barrier penetration (BPM) is shown by the dotted curve, coupled-channel calculation including inelastic excitation (IE) of the projectile and target by the dashed curve, coupled-channel calculation including inelastic excitation and transfer (nXFR) by the dashed-dotted curve, and microscopic model (SEDF) by the solid curve.

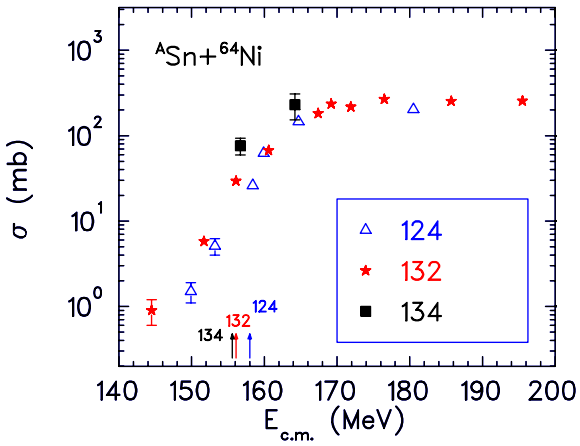

FIGURE 5. Comparison of ER cross sections for ^{134}Sn+^{64}Ni (filled squares), ^{132}Sn+^{64}Ni (filled stars), and ^{124}Sn+^{64}Ni (open triangles). The vertical bars are the barrier height of the three reactions.

value increases as the number of neutrons in the Sn isotope increases. This is consistent with the fact that the fission barrier height increases as the neutron excess in the compound nucleus increases. The reduced ER cross section as a function of the average mass of the ER, calculated by the statistical model code PACE2, is shown in Fig. 6(b). For the compound nucleus made with Sn isotopes of mass number greater than 120, neutron evaporation is the dominant particle decay mode and Pt isotopes are the primary ERs. For ERs made with the same Sn isotope, the higher mass ones are formed at lower beam energy and lower excitation energy. Although the mass of the compound nucleus is different with different Sn isotopes, the ER can be the same if a different number of neutrons is emitted. Moreover, for a Sn mass greater than 120, the reaction with a more neutron-rich Sn produces the same Pt isotope at a higher rate.

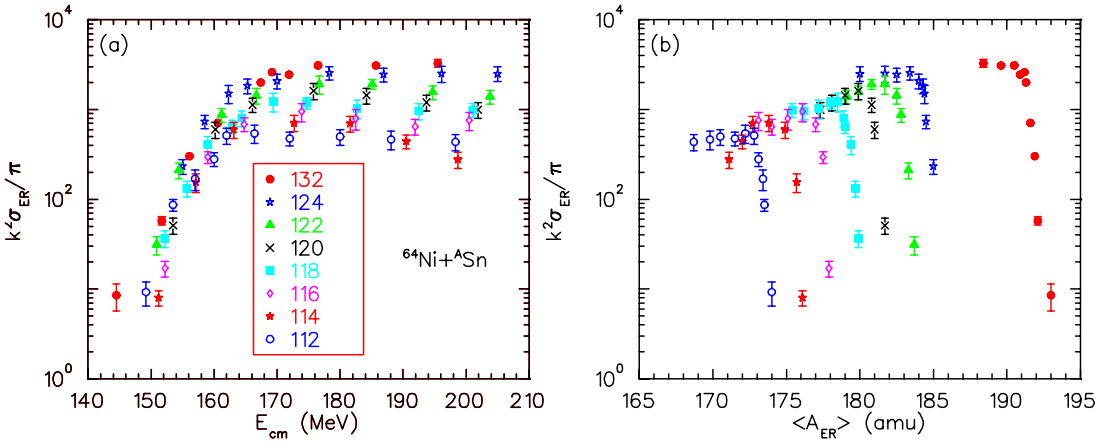

FIGURE 6. Reduced ER cross sections for ^{A}Sn+^{64}Ni as a function of (a)center of mass energy and (b)average mass of the ERs.

The ^{132}Sn and ^{64}Ni fusion experiment is extended to the use of ^{134}Sn as the projectile. The binding energy of ^{134}Sn is 3.7 MeV, approximately half the value of ^{132}Sn. The number of neutron-transfer channels with positive Q-values is a factor of two greater than for the ^{132}Sn+^{64}Ni reaction. The preliminary result of the measurement is shown in Fig. 5. The fusion of ^{134}Sn+^{64}Ni appears to be enhanced compared to that of ^{124,132}Sn+^{64}Ni after considering the effect of nuclear sizes. However, it is conceivable that the surface of ^{134}Sn is more diffuse because of its low neutron binding energy. The nuclear radius and the interaction barrier calculated with systematics obtained from stable nuclei may not be valid.

The ^{132}Sn beams were purified by a chemical method to reduce the isobaric contaminants[18]. The beams consist of $\sim$96 % of ^{132}Sn and a small amount of ^{132}Te. Since Te has a higher Coulomb barrier and fusion is suppressed, its contribution to the measurement can be ignored. However, for the ^{134}Sn beam even with chemical purification, the intensity of ^{134}Sb and ^{134}Te is still fairly high. Their contribution to the measurement cannot be ignored. The ER excitation function of ^{134}Te+^{64}Ni has been measured separately because a high purity ^{134}Te beam can be produced. However, a high purity ^{134}Sb beam is not available at present. The ^{134}Sn results shown in Fig. 5 have subtracted the contribution from ^{134}Te but not ^{134}Sb. Furthermore, the concentration of all the mass 134 isobars varies with the ion source operating conditions. This further complicates the data analysis. More details of the ^{134}Sn work can be found in the contribution by D. Shapira in this conference[19].

II. ^{96}Zr target

Sahm *et al.* reported that the extra-push energy increases as the neutron excess of Zr increases in ^{124}Sn+^{90,92,94,96}Zr fusion[20]. This is contrary to the expectation that the extra-push energy decreases as the neutron excess of the compound nucleus increases. However, their conclusions were drawn from the measurement of very small ER cross

sections (μb) with uncertainties greater than 30% to deduce the fusion probability.

An Oregon State University group measured the fusion-fission cross sections of ^{124,132}Sn+^{96}Zr[21]. The excitation functions for the two reactions are compared in Fig. 7. The cross sections for ^{132}Sn induced fusion are less than those for ^{124}Sn induced fusion at high energies. At low energies, a surprisingly large fusion enhancement was observed for ^{132}Sn+^{96}Zr. This result is very preliminary. The measurement with ^{124}Sn has been repeated to evaluate possible systematic errors and the data analysis is in progress. The ^{132}Sn and ^{96}Zr fusion experiment will be repeated in the near future.

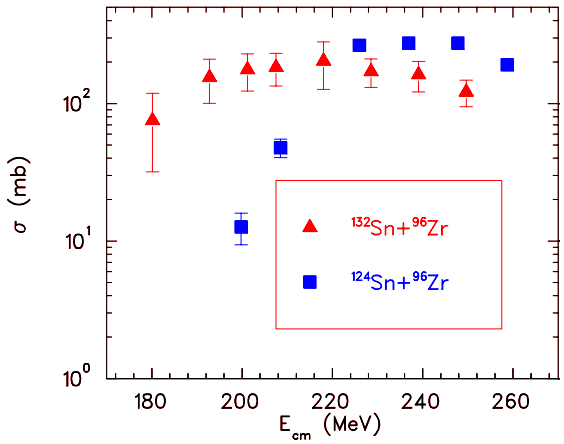

FIGURE 7. Preliminary results of fission excitation functions for ^{132}Sn+^{96}Zr (triangles) and ^{124}Sn+^{96}Zr (squares).

DISCUSSION

Beams obtained by high energy projectile fragmentation can be very short-lived compared to those produced by the isotope separation on-line method. They offer the opportunity to study fusion with nuclei very far from the stability. However, it is necessary to improve the beam quality significantly. For instance, the beam can be degraded to the desired energies and cleaned up with slits and optical elements before delivering to the target chamber in the ^{38}S experiments. This may enable measurements to be carried out at sub-barrier energies. Additionally, it would be very interesting to use such beams to measure ER cross sections. Because the measurement would be performed near zero degrees, the presence of scattered beams in the background will limit how well the ERs can be identified and how low the cross sections can be measured. It is very crucial to have high quality beams.

High purity beams are desirable for fusion measurements. Sometimes, isobar contamination is unavoidable even with the use of chemical purification techniques and sophisticated separators. However, it has been demonstrated that beam tracking is a promising way to deal with such problems[22].

SUMMARY AND OUTLOOK

To this day, fusion experiments performed with medium-mass RIBs are scarce. In most cases, the observed fusion enhancement can be accounted for by the larger radius of the radioactive nuclei lowering the barrier. Perhaps ^{134}Sn induced fusion is an exception. Further measurement and analysis are required to determine if sub-barrier fusion is enhanced by effects other than the change in nuclear sizes.

In order to find a systematic behavior of fusion induced by RIBs, experiments with a variety of beams are required. Several upgraded facilities are scheduled to be in operation in the near future and a few next generation facilities are under consideration. It is expected that more fusion measurements will be carried out with medium-mass RIBs and progress will be made towards understanding the mechanisms of fusion involving short-lived nuclei.

ACKNOWLEDGMENTS

The author wishes to thank D. Shapira, W. Loveland, and A. M. Vinodkumar for providing their data and discussions. Research at the Oak Ridge National Laboratory is supported by the U.S. Department of Energy under contract DE-AC05-00OR22725 with UT-Battelle, LLC.

REFERENCES

1. V. Yu. Denisov, *Eur. Phys. J. A* **7** 87 (2000).
2. V. I. Zagrabaev, *Phys. Rev. C* **67**, 016101(R) (2003).
3. J. F. Liang and C. Signorini, *Int. J. Mod. Phys. E* **14**, 1121 (2005).
4. J. F. Liang *et al.*, *Phys. Rev. Lett.* **91**, 152701 (2003).
5. Y. X. Watanabe *et al.*, *Eur. Phys. J.* **A10**, 373 (2001).
6. W. Loveland *et al.*, submitted to *Phys. Rev. C*.
7. K. E. Zyromski *et al.*, *Phys. Rev. C* **55**, R562 (1997).
8. K. E. Zyromski *et al.*, *Phys. Rev. C* **63**, 024615 (2001).
9. M. B. Tsang *et al.*, *Phys. Rev. C* **28**, 747 (1983).
10. B. B. Back *et al.*, *Phys. Rev. C* **31**, 2104 (1985).
11. A. Gavron, *Phys. Rev. C* **21**, 230 (1980).
12. K. Hagino, N. Rowley, and A. T. Kruppa, *Compu. Phys. Commun.* **123**, 143 (1999).
13. R. A. Broglia and A. Winther, *Heavy Ion Reactions, Frontiers in Physics Lecture Note Series*, Vol. **84** (Addison-Wesley, Redwood City, CA, 1991).
14. M. Liu *et al.*, *Nucl. Phys.* **A768**, 80 (2006).
15. K. T. Lesko *et al.*, *Phys. Rev. C* **34**, 2155 (1986).
16. R. Bass, *Nucl. Phys.* **A231**, 45 (1974).
17. W. S. Freeman *et al.*, *Phys. Rev. Lett.* **50**, 1563 (1983).
18. D. W. Stracener, *Nucl. Instrum. and Methods* **B204**, 42 (2003)..
19. D. Shapira *et al.*, contribution in this proceedings.
20. C.-C. Sahm *et al.*, *Nucl. Phys.* **A411**, 316 (1985).
21. A. M. Vinodkumar, private communication.
22. D. Shapira *et al.*, *Nucl. Instrum. and Methods* **A490**, 159 (2002).